THERMALLY INDUCED OPTICAL PHASE CONJUGATION BY DEGENERATE FOUR-WAVE MIXING

B. RAGHAVENDRA PRASAD, R. KRISHNA MOHAN, P. S. NARAYANAN, C. K. SUBRAMANIAN and P. CHANDRA SEKHAR
Department of Physics, Indian Institute of Science, Bangalore 560 012, India.

ABSTRACT

Thermally induced optical phase conjugation by degenerate four-wave mixing (OPC-DFWM) offers considerable scope for high power adaptive optics applications. A detailed study of the optical phase conjugation in solutions of Rhodamine 6G and Rhodamine B in acetone, ethanol, methanol and water has been made with second harmonic 532 nm radiation of Nd : YAG under near zero time delay conditions. Reflectivity up to 50% has been obtained and as expected from theory, Rh6G and RhB both show a much larger reflectivity in acetone than in the other solvents due to the Q factor and higher thermalization yield in acetone. The dependence of reflectivity on the angle of interaction and the pump and probe beam intensities are also reported. The autotracing and "healing" property of OPC are demonstrated with photographs of the original, distorted and corrected beams.

INTRODUCTION

Optical phase conjugation (OPC) has been obtained by the use of several nonlinear optical effects, to exactly reverse both the direction of propagation and the overall phase factor of a coherent beam of light. This wavefront or phase reversal of an electromagnetic wave is equivalent to performing an operation of complex conjugation of the complex spatial amplitude. This phenomenon has been observed with all states of matter utilizing various nonlinear optical effects viz. stimulated Brillouin scattering[1], three-wave mixing[2–4], four-wave mixing[5–8], photon echoes[9,10], surface effects[11,12], non-local field effects[13], etc. An extensive overview of various techniques mentioned above and their applications can be found in Fisher[14], Zeldovich *et al*[15] and Pepper[16].

Initially Caro and Gower[17] and later Gower[18] attempted to give a theoretical model for thermally-induced degenerate four-wave mixing (DFWM) in absorbing media. Even though they could satisfactorily take account of many parameters governing the phase conjugate reflectivity (PCR), the influence of important parameters relating to different time-scales involved in grating formation and decay was not clearly elucidated. Hoffman[19], on the other hand, gave a more detailed theoretical model based on coupled hydrodynamic equations which include the time-scale parameters unexplained hitherto.

The generation of phase conjugate signals, by the technique of formation of thermal gratings in absorbing media especially of dye solutions, has been shown to have several advantages. Thermal gratings are generated in a variety of media where absorption of light causes transitions in the molecules of the media. Subsequent local heating or thermalization by radiationless relaxation of the optically excited molecules gives rise to periodic temperature (or entropy) fluctuations in some cases and density fluctuations in others. These result in a spatial modulation of the refractive index of the solvent which then acts as a phase grating in the scattering of incident light. Generally the scattering by temperature or entropy fluctuations is termed as stimulated thermal Rayleigh scattering and scattering of light by density fluctuations is termed as stimulated thermal Brillouin scattering[20,21].

The use of dye solutions as nonlinear media for quantum electronics was originally based on the effect of saturation of their absorptivity in powerful radiation fields. Most of the experiments on OPC-DFWM in dyes show that pure thermal effects play a major role in the recording of the interference pattern, particularly if the absorbed energy relaxes into heat immediately. The spatially inhomogeneous heat release leads to inhomogeneous changes in permittivity. The nature of such disturbances largely depends on the relationship between pulse duration and the characteristic time scales of different physical processes in the medium.

Theory

The first theoretical model for stimulated scattering of light was given by Batra *et al*[21]. Hoffman[19] based her investigations on this approach and

extended it to thermally-induced DFWM. In Hoffman's[19] approach, the dynamics of the thermal grating formation is modelled in terms of a set of three coupled hydrodynamic equations describing the behaviour of the medium in the presence of an electromagnetic field. Then Maxwell's wave equation is added to describe the behaviour of the system in the presence of appropriate nonlinear polarization.

In equation (1) below, the absorption of electromagnetic energy by dye molecules is taken into account in the first term, which subsequently is transferred via thermalization to the host medium or solvent. The rate of change of internal energy density $U(t)$ can therefore be written as:

$$\frac{\partial U}{\partial t} = \frac{nc\,\alpha E^2}{4\pi} + D\frac{\partial^2 U}{\partial Z^2} - \frac{U}{\tau_{\text{eff}}}, \qquad (1)$$

where, n is the refractive index, c, the speed of light in vacuum, α, the linear absorption coefficient, E, the total electric field, D, the diffusion constant, and τ_{eff}, the thermalization time. The first term on the right side which describes the absorption of electromagnetic energy by the dye molecules is taken to be instantaneous. The second term describes the diffusion of these excited molecules, which gives rise to 'nonlocal' heating. The last term describes the loss of energy via collisions by the excited molecules to the host medium.

The other two coupled hydrodynamic equations are:

$$\rho_0 C_v \cdot \frac{\partial T_1}{\partial t} - K\frac{\partial^2 T_1}{\partial Z^2} - \frac{T_0 F}{\rho_0}\frac{\partial \rho_1}{\partial t} = \frac{U}{\tau_{\text{eff}}} \qquad (2)$$

$$\frac{\partial^2 \rho_1}{\partial t^2} - \frac{B^T}{\rho_0}\frac{\partial^2 \rho_1}{\partial Z^2} - \frac{\eta}{\rho_0}\frac{\partial}{\partial t}\left(\frac{\partial^2 \rho_1}{\partial Z^2}\right) - F\left(\frac{\partial^2 T_1}{\partial Z^2}\right) = -\frac{\gamma^e}{8\pi}\frac{\partial^2 (E^2)}{\partial Z^2}, \qquad (3)$$

where ρ_0 and T_0 are the equilibrium values of density and temperature, C_v, the specific heat at constant volume, terms with T_1 and ρ_1 are the fluctuations in temperature and density, K, the thermal conductivity, F, the coupling constant between density and temperature fluctuations, B^T, the isothermal bulk modulus, η, effective viscosity describing the damping process, and γ^e, the electrostrictive constant.

Equation (2) is a heat diffusion equation with an additional heat source term. It describes the thermal fluctuations in the medium resulting from the thermalization of the optically excited molecules. The first two terms predict that the amplitude of a temperature fluctuation occurring in the medium decays exponentially in time. The terms involving F in (2) and (3) describe the coupling between temperature and density. The right side term of (2) is the heat source term arising from the thermalization of the optically excited molecules. Equation (3) describes the density fluctuations due to the thermalization process by the coupling term and by the direct electrostrictive force contribution due to the electromagnetic field.

A detailed analysis assuming the slowly varying approximation for the amplitudes of the thermodynamic quantities[22] then provides us with an expression for the phase conjugate amplitude as given below:

$$A_4(Z=0,t) = \frac{i\omega(\partial\varepsilon/\partial T)_p}{16\pi\rho_0 C_p \tau_{\text{eff}}}\,[1-\exp(-\alpha L)] \exp\left[\frac{\alpha L}{2}(1-\cos\theta)\right] A_2(t)\,F(t), \qquad (4)$$

where $(\partial\varepsilon/\partial T)_p$ is the change in dielectric constant with temperature at constant pressure, ρ_0 and C_p are the density and specific heat at constant pressure of the solvent respectively, α, the absorption coefficient, L, the interaction length and, θ the interaction angle.

The reflectivity of the process can then be calculated from conventional definition

$$R = \exp(-\alpha L)\,\frac{\int |A_4|^2\,dt}{\int |A_3|^2\,dt}, \qquad (5)$$

where A_4 and A_3 are the phase conjugate and the probe beam amplitudes respectively.

As shown by the above expression, R involves a triple integration in time over the laser pulse duration modified by time evolution functions appropriate to the thermal gratings. By assuming rectangular pulse shapes for the electric field amplitudes, an approximate analytical expression for reflectivity R is finally obtained as:

$$R = f^2 Q^2 \exp\left(\frac{-\alpha L}{\cos\theta}\right)[1-\exp(-\alpha L)]^2 I_1 I_2 G(t_D), \qquad (6)$$

where

$$Q = \frac{2\pi(\mathrm{d}n'/\mathrm{d}T)}{\lambda\rho_o C_p} \tag{7}$$

$$G(t_D) = \frac{1}{\tau_{\mathrm{eff}}^2 t_p'} \int^{t_D+t_p} \mathrm{d}t\, F^2(t, T), \tag{8}$$

and

$$F(t, T) = \frac{1}{\Gamma_u} \int_0^T \mathrm{d}t' \,[1-\exp(-\Gamma_u t')] \ldots$$

$$\ldots \{\exp[-(t_p-t_p')/\tau_R] - \exp[-\Gamma_B/2(t_p-t_p')]. \cos\beta_B(t_p-t_p')\}. \tag{9}$$

In (6), I_1 and I_2 are the pump and the read beam intensities, f is the phenomenological factor defined as the fraction of the absorbed light energy converted into heat[23,24].

In (9), $1/\Gamma_u$ is the thermalization time due to non-instantaneous and non-local solute solvent energy transfer, Γ_B is the full Brillouin line width, β_B is the coefficient of volume expansion, t_P and t_P' are the probe and phase conjugate pulse widths respectively and τ_R is the Rayleigh lifetime or thermal grating decay time.

The term $G(t_D)$ given in (6) contains the details of thermal grating build-up and decay where t_D represents the time delay of the backward propagating 'read' beam with respect to the forward propagating pump and probe beams. An approximate expression for $G(t_D)$, for very short time delay region i.e. $t_D \ll t_p - t_p'$ is given as[25,26]

$$G(t_D) \simeq \frac{t_p'^2}{3\tau_{\mathrm{eff}}^2\,\Gamma_u^2}\left[1 + \frac{3t_D(t_D+t_p')}{t_p'^2}\right], \tag{10}$$

where $$\tau_{\mathrm{eff}}\,\Gamma_u = 1 + \tau_{\mathrm{eff}}\,Dq^2, \tag{11}$$

where, τ_{eff} is effective thermalization time, D, the thermal diffusion time constant for the dye molecules in the solvent and q, the thermal grating wavevector given by $q = 2k\sin(\theta/2)$ where $k = n\,\omega/c$.

The simplified expressions given above are rendered valid by a careful choice of parameters in accordance with the conditions prevailing in the specific experimental situations of interest. All the time scales that are involved can be classified as those that characterize the medium and those that characterize laser parameters. The information regarding the thermal grating formation and decay can be predicted by the relationships between them. In this theory a simple model for the energy levels of the solute is assumed. The complex time-dependent effects of fluorescence have been ignored. These introduce some uncertainty in the exact determination of the diffusion constant and thermalization time. Most of the absorbing molecules cannot be represented by a simple two-level systems. A more complete description of the solute-solvent interaction has to consider details of the contributions due to rotational, vibrational and electronic nonradiative relaxation, and also the longlived excited state decay. The inclusion of these parameters depends also on the solute under consideration. All these mechanisms play an important role when integrated reflectivities are deduced as a function of read beam time delay.

EXPERIMENT

For applications where high overall phase conjugate efficiencies are required, nonlinear media with highest possible third order susceptibilities are needed. In practice for fixed experimental parameters such as the laser wavelength and pulse characteristics, requirements like the material speed of response and damage threshold impose constraints on the choice of the medium. The availability of a suitable material, the choice of wavelengths, ease of operation, high overall system efficiency, etc. render the organic dye solutions attractive for phase conjugate wave generation. An added advantage with dye solutions is that the nonlinear effect can be obtained over a wide range of wavelengths from 300 to 1100 nm by the process of absorption of light by organic dyes in appropriate fluorescence quenching solvents to maximize local heating and causing a refractive index change, as described earlier.

For optimal thermal grating efficiencies a careful choice of the laser and medium time scales has to be made as is evident from the theory outlined above. The influence of solvent-dye combinations, geometrical arrangements, read beam time delays, laser pulse durations, the angle of interaction between the pump or write and the probe beams, the proper concentration-interaction length product for the chosen dye system and the system geometry and optimum beam intensities to avoid saturation and spurious scattering effects must all be considered carefully for higher phase conjugate reflectivities. A systematic study of thermally induced DFWM in dye solutions has therefore been taken up by us.

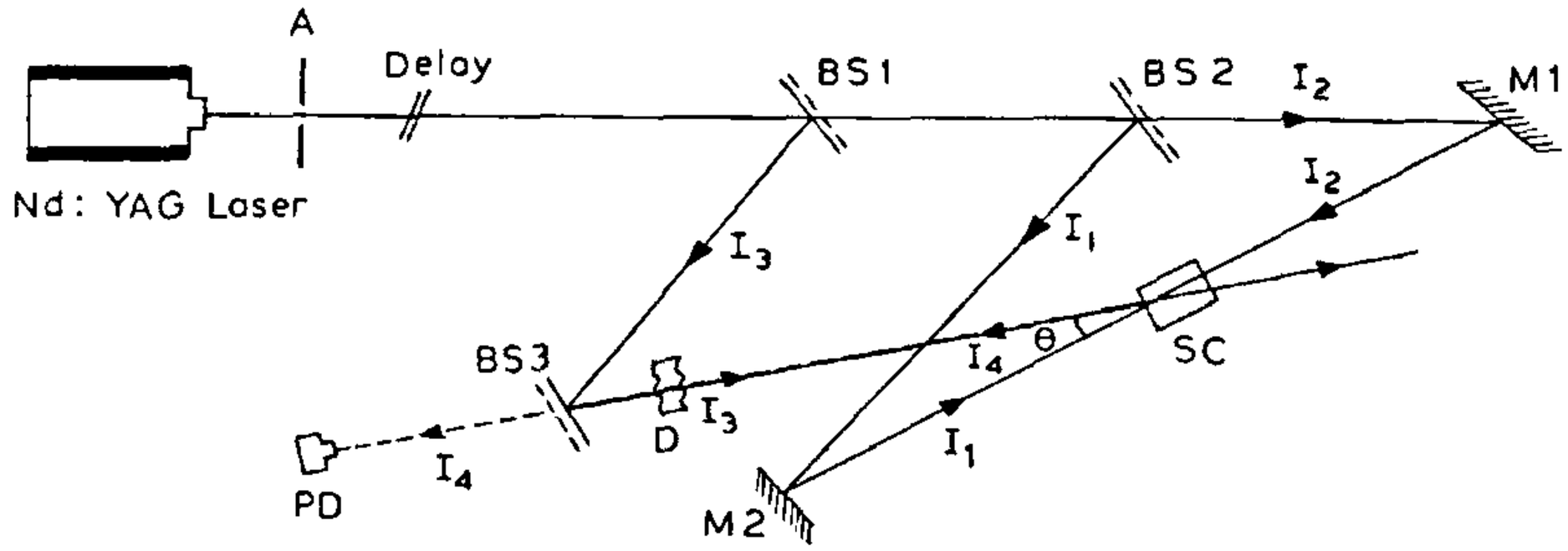

Figure 1. Experimental set-up of optical phase conjugation by degenerative four wave mixing. [I_1–Pump beam, I_2–Read beam, I_3–Probe beam, I_4–Phase conjugate beam, BS–Beam splitter, SC–Sample cell, PD–Photo detector, D–Phase distorter, A–Aperture, M–Mirror.]

The experimental investigations are aimed at studying the concentration effect on the reflectivity, the influence of various dye-solvent systems, the dependence on the writing or the interaction angle and the variation of reflectivity with the beam intensities. The experiments were conducted using the second-harmonic of the Nd : YAG laser i.e. at 532 nm with filled in beam configuration. The pulse duration is between 6 and 8 ns and the peak power used for the experiments was about 15 MW per pulse.

The experimental set-up used is shown in figure 1. The incident laser beam is split into two vertically (or s−) polarized beams by the beam-splitter BS1 with a reflectivity of 10% . The transmitted beam is then split into two beams of equal intensity by the 50% beam-splitter BS2. The beam transmitted by BS2 is reflected on to the sample cell SC by a mirror M1. This beam is the backward propagating or the 'read' beam. The beam reflected by BS2 is in turn reflected on to the sample cell by a mirror M2. This beam is referred to as the forward propagating 'pump' or 'write' beam. These two beams are made collinear and counter-propagating by a careful adjustment of the mirrors M1 and M2. The reflected beam from the beam-splitter BS1 is further split by a 30% reflecting beam-splitter BS3 to maintain a high pump-probe ratio. The beam reflected by BS3 is designated as the forward propagating 'probe' beam which is made to interact with the pump beam in the sample cell to form the thermal grating. It is mandatory to satisfy the coherence requirement for the two beams forming the grating by adjusting the path lengths of both the beams. The arrangement was such that the interaction angle could be varied from 10 to about 45°. The beam intensities and the pulse widths at various stages in the set-up were monitored by photodetectors *PD*.

RESULTS AND DISCUSSION

From the expression for phase conjugate reflectivity, we can obtain the optimum concentration-interaction length product by maximizing the phase conjugate reflectivity. A straightforward analysis with small angle approximation shows that reflectivity is maximum at $\alpha L = 1.1$ and falls off on either side, provided the other parameters like pump-probe ratio, dye solvent combination, angle of interaction, etc. are unchanged. The values of various constants used in calculations are given in table 1. The results obtained for different combinations of dyes Rhodamine 6G and Rhodamine B in

Table 1 *Physical constants of various solvents*

Solvent	Refractive index (n)	$[dn/dt]_p$ (1exp−5/K)	Density (g/cc)	Sp. heat at const. pres. (J/g.K)
Water	1.33299	−8	1.00	4.182
Methanol	1.33118	−36	0.7961	2.51
Ethanol	1.36018	−40	0.7893	2.43
Acetone	1.35746	−53	0.792	2.21

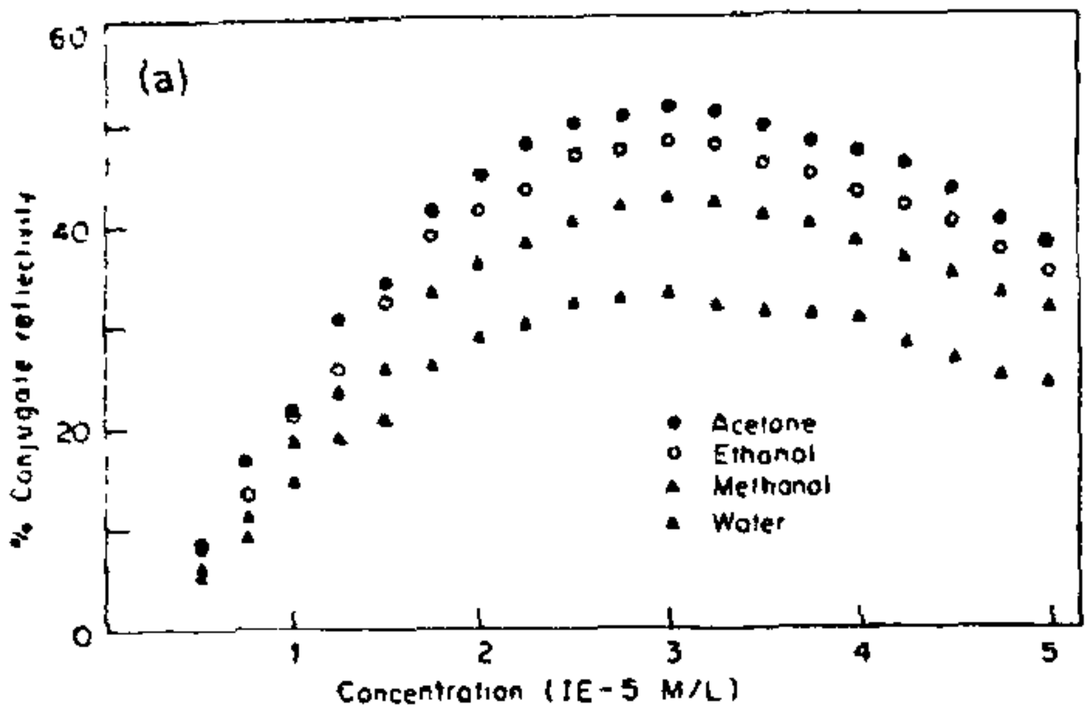

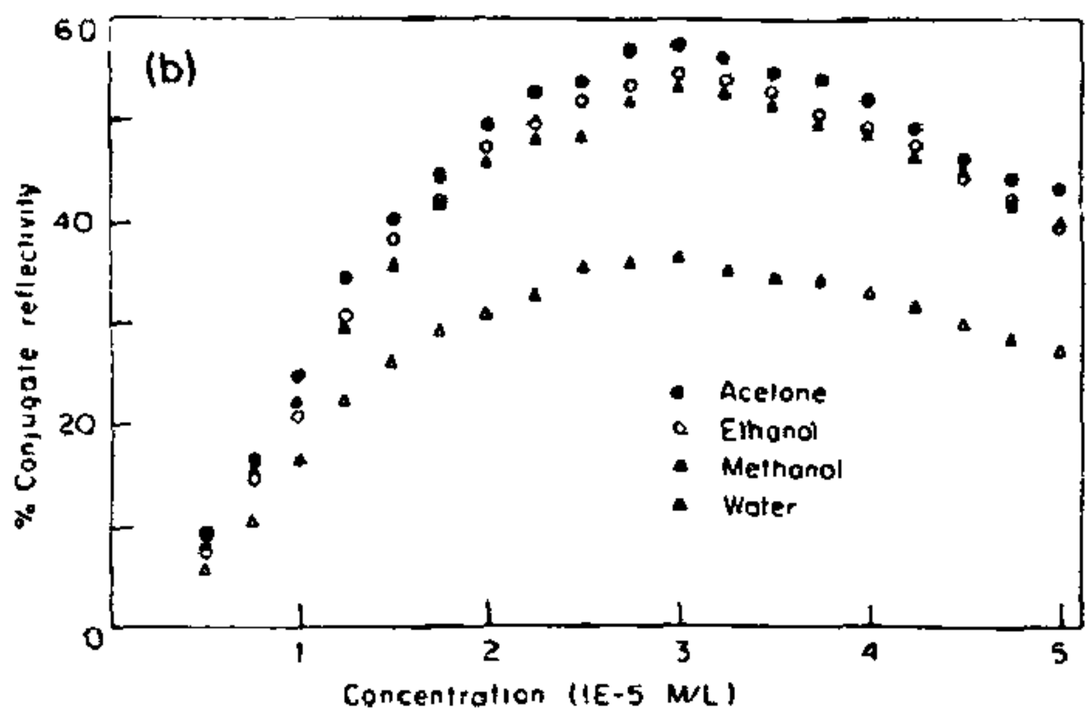

Figure 2a,b. Concentration dependence of phase conjugation reflectivity. Angle of interaction = 10°. **a.** Rhodamine −6G in water, methanol, ethanol and acetone, and **b.** Rhodamine B in water, methanol, ethanol and acetone.

solvents like acetone, ethanol, methanol and water are shown in figures 2a and 2b.

The results shown in the figures confirm that the system conforms to the functional form of the theoretical result of Hoffman. An interesting observation is the much larger conjugate reflectivity for both Rhodamine 6G (Rh6G) and Rhodamine B (RhB) in acetone for the same dyes in other solvents. This is obviously due to the Q^2 factor, and in particular the larger dn/dt value of acetone and also possibly to higher thermalization yields in acetone.

The higher overall conjugate reflectivity in case of RhB over that of Rh6G in all solvents has to be correlated with the fact that the RhB molecules fluoresce less efficiently implying that only a smaller fraction of the laser energy is "wasted" on radiative relaxation instead of the desired thermalization. Earlier reports[27] regarding the quantum efficiency of fluorescence show that Rh6G gives typically 40% fluorescence yield, which is higher than that of RhB.

The present observations of the dependence of the reflectivity on the angle of interaction are shown in figure 3. From the expression for reflectivity (equation (6)), the angular part can be separated at small time delay region and the equation can be rewritten as

$$R = \frac{A \exp(-\alpha L/\cos\theta)}{(1 + B \sin^2\theta/2)^2} \qquad (12)$$

where

$$A = f^2 Q^2 I_1 I_2 \left[\frac{t_p'^2}{3} + t_D(t_D + t_p') \right]$$

$$[1 - \exp(-\alpha L)^2]$$

and

$$B = \frac{16 \pi^2 \tau_{\text{eff}} Dn^2}{\lambda^2} .$$

The experimental results obtained for Rh6G in acetone are shown in figure 3. This behaviour i.e. the decrease of reflectivity with increasing angle of interaction is in general agreement with expression (12).

The variation of the conjugate reflectivity with pump and probe intensities was also studied and the results are shown in figure 4a–d. The ratio of the pump-to-probe intensity was maintained at about 25. The reflectivities are plotted against incident intensity given as lamp joules. As an accurate power meter which could measure high powers was not available we have chosen lamp joules, as indicated on the laser panel, as the units for representing the intensity. As is evident from the graphs the reflectivity increases linearly with increasing pump and probe intensities in all solvents. But the behaviour in acetone and ethanol is significantly different from that in methanol and water. The reflectivity of Rh6G in methanol and water increases slowly compared to that of RhB in these solvents at all incident intensities. But reflectivity of Rh6G in

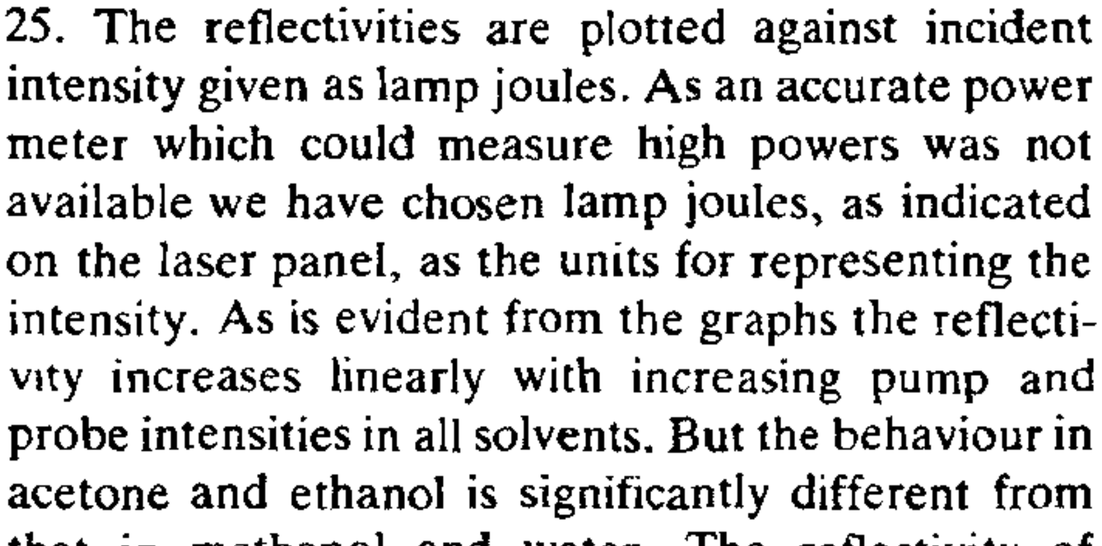

Figure 3. Dependence of phase conjugation respectivity on angle of interaction for Rh6G-Methanol system, $\alpha L \simeq 1$.

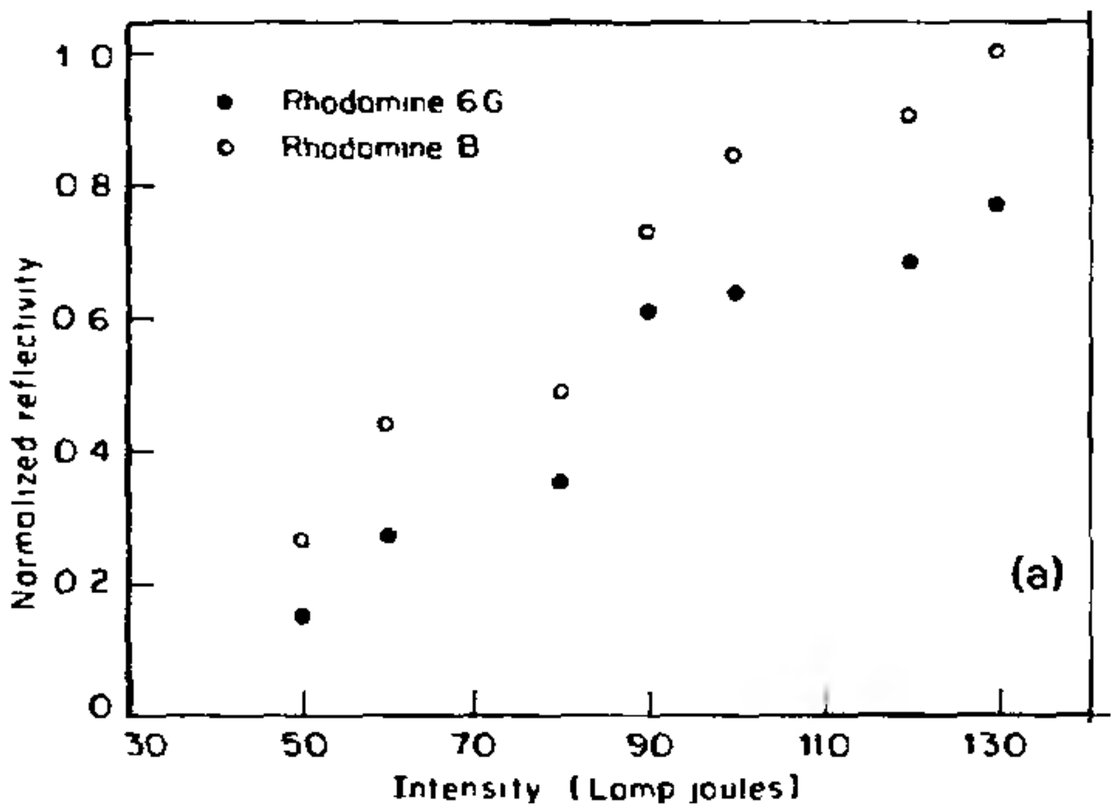

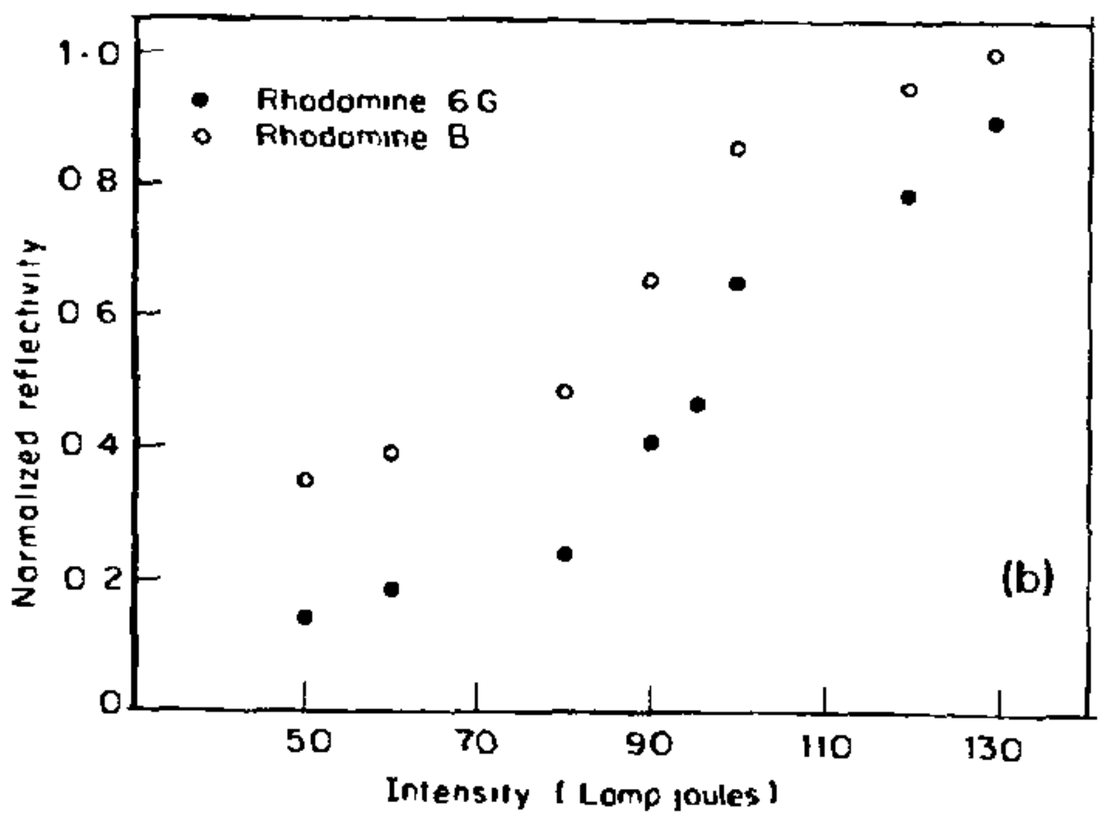

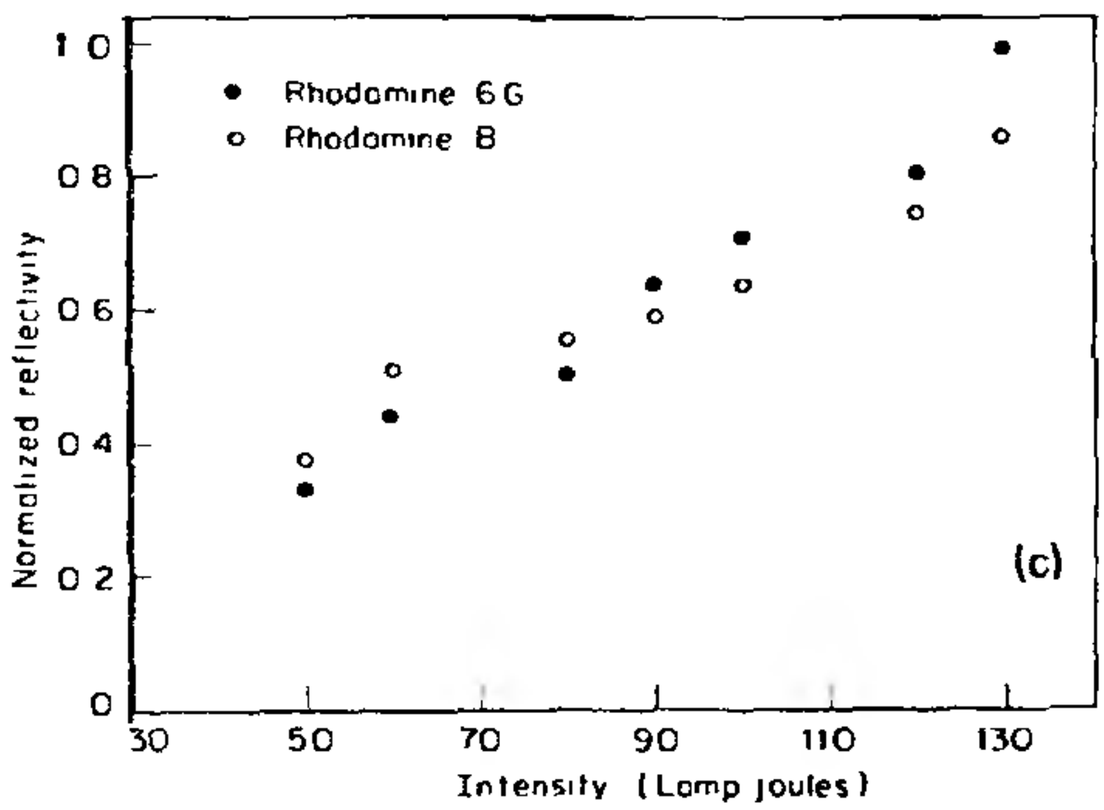

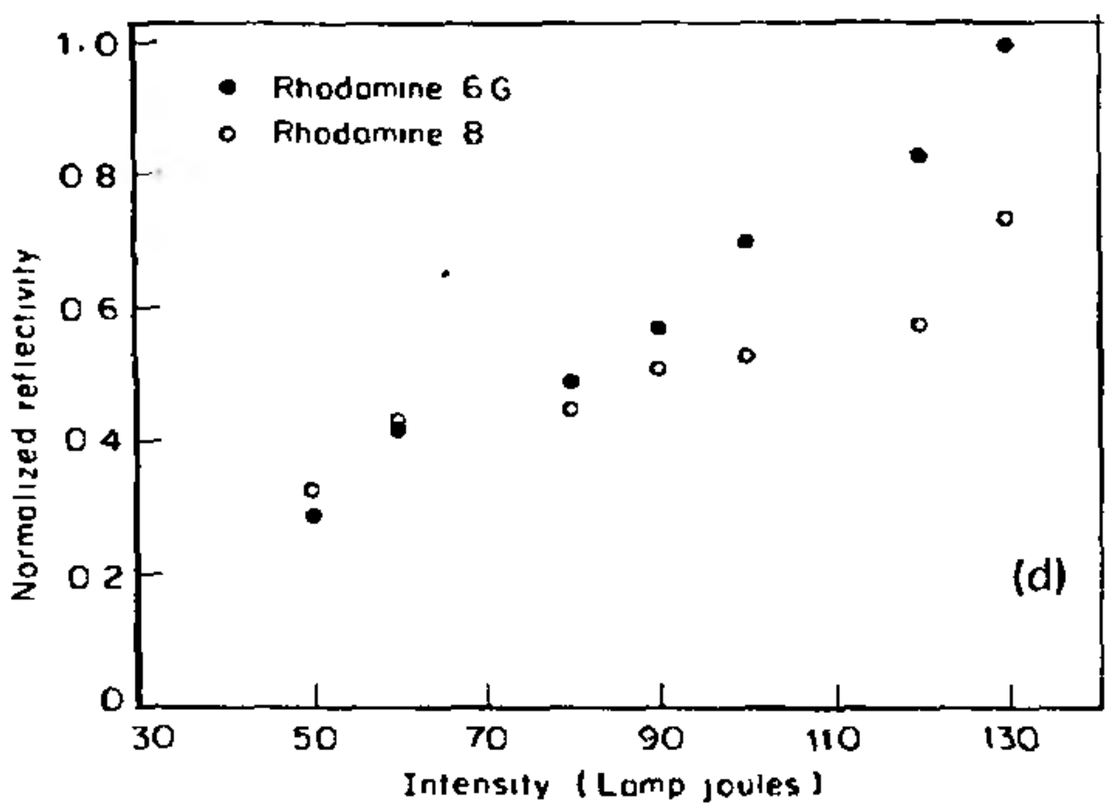

Figure 4a–d. Intensity dependence of phase conjugate reflectivity for Rh6G, and RhB in various solvents: **a.** Water (normalized with respect to RhB); **b.** Methanol (normalized with respect to RhB); **c.** Ethanol (normalized with respect to Rh6G), and **d.** Acetone (normalized with respect to Rh6G).

acetone and ethanol is less than that of RhB in the same solvents at low intensities and exceeds the RhB reflectivity at higher intensities. This marked deviation in case of ethanol and acetone suggests that saturation effects commence at higher probe and pump intensities. This trend is even more noticeable at very high power densities, obtained by focusing the pump and read beams onto the sample cell, except that this configuration is not congenial for efficient phase conjugate wave generation.

Figure 5a,c. Distortion correction properties of Phase Conjugate Beam. **a.** Phase conjugate beam; **b.** Probe beam after single passage through the phase distorter, and **c.** Conjugate beam after reverse passage through the phase distorter.

The autotracing property of phase conjugation has many potential applications in problems associated with the propagation of high quality optical beams through distorting media. This property of distortion correction has been observed (figure 5). Figure 5a depicts the phase conjugate beam without any aberrator in the path of the probe beam. Figure 5b shows the probe beam after a single passage through the phase distorter placed in its path. Figure 5c is the phase conjugation beam after the reverse passage through the phase distorter. These pictures conclusively prove that optical phase conjugation can be applied to overcome problems connected with propagation of optical beams through distorting media. These photographs were taken using a Linhof Technica camera.

In conclusion, the thermal mechanism not only offers scope for application of phase conjugation through DFWM, but provides a powerful method of studying the energy transfer processes between absorbing molecules like the dyes and the solvent media in various time scales characteristic of different processes. Further investigations along these lines on DFWM are in progress.

ACKNOWLEDGEMENTS

The entire work and the setting up of the laser laboratory were with financial support from the Defence Research and Development Organization (Research and Training Programme). We thank the DRDO and IISc for enabling us to carry out these investigations.

18 December 1987; Revised 17 February 1988

1. Zeldovich, B. Ya., Popovichev, V. I., Regulskii, V. V. and Fasisulla, F. S., *JETP. Lett.*, 1972, **15,** 109.
2. Yariv, A., *J. Opt. Soc. Am.*, 1976, **66,** 301.
3. Yariv, A., *Appl. Phys. Lett.*, 1976, **28,** 88.
4. Yariv. A., *Opt. Commun.*, 1977, **21,** 49.
5. Yariv, A. and Pepper, D. M., *Opt. Lett.*, 1977, **1,** 16.
6. Bloom, D. M. and Bjorklund, G. E., *Appl. Phys. Lett.*, 1977, **31,** 59.
7. Jensen, S. L. and Hellwarth, R. W., *Appl. Phys. Lett.*, 1978, **32,** 166.
8. Hellwarth, R. W., *J. Opt. Soc. Am.*, 1977, **67,** 1.
9. Griffen, N. C. and Heer, C. V., *Appl. Phys. Lett.*, 1978, **33,** 86.
10. Voronoin, E. S., Ivakhnik, V. V., Petnikova, V. M., Solomatin, V. S. and Solonov, V. V., *Sov. J. Quantum Electron.*, 1979, **9,** 769.
11. Golubstov, A. A., Pilipeteskii, N. F., Sudarkin, A. N. and Shkunov, V. V., *Sov. J. Quantum Electron.*, 1981, **11,** 402.
12. Kulikov, O. L., Pilipeteski, N. F., Sudarkin, A. N. and Shkunov, V. V., *JETP Lett.*, 1980, **31,** 345.
13. Gunter, P., *Phys. Rep.*, 1982, **93,** 199.
14. Fisher, R. A. (ed.), *Optical phase conjugation*, Academic Press, New York, 1983.
15. Zel' dovich, B. Ya., Pilipeteskii, N. F., Shkunov, V. V., *Principles of phase conjugation*, Springer Verlag, Berlin, 1985.
16. Pepper, D. M., *Opt. Eng.*, 1982, **21,** 156.
17. Caro, R. G. and Gower, M. C., *IEEE J. Quantum Electron.*, 1982, **QE-18,** 1376.
18. Gower, M. C., *Prog. Quantum Electron.*, 1984, **9,** 101.
19. Hoffman, H. J., *IEEE J. Quantum Electron.*, 1986, **QE-22,** 552.
20. Herman, R. M. and Gray, M. A., *Phys. Rev. Lett.*, 1967, **11,** 324.
21. Bathra, I. P., Enns, R. H. and Pohl, D., *Phys Status Solidi*, 1971, **48,** 11.
22. Pohl, D. and Kaiser, D., *Phy. Rev.*, 1970, **B1,** 31.
23. Tocho, I. O., Sibbette, W. and Bradley, D. J., *Opt. Commun.*, 1980, **34,** 12.
24. Tocho, I. O., Sibbette, W. and Bradley, D. J., *Opt. Commun.*, 1981, **37,** 67.
25. Hoffman, H. J. and Perkins, P. E., *IEEE J. Quantum Electron.*, 1986, **QE-22,** 563.
26. Hoffman, H. J., *J. Opt. Soc. Am.*, 1986, **B3,** 253.
27. Phillion, B. W., Kuizeuga, D. J. and Siegman, A. E., *Appl. Phys. Lett.*, 1975, **27,** 85.